2026 IEEE International Conference on Robotics and Automation (ICRA 2026)
June 1-5, 2026. Vienna, Austria

Orbital Stabilization and Time Synchronization of Unstable Periodic Motions in Underactuated Robots

Maksim Surov[1], Maksim Grigorov[1], Sergei Gusev[1], Oleg Sumenkov[1]

***Abstract*— This paper presents a control methodology for achieving orbital stabilization with simultaneous time synchronization of periodic trajectories in underactuated robotic systems. The proposed approach extends the classical transverse linearization framework to explicitly incorporate time-desynchronization dynamics. To stabilize the resulting extended transverse dynamics, we employ a combination of time-varying LQR and sliding-mode control. The theoretical results are validated experimentally through the implementation of both centralized and decentralized control strategies on a group of six Butterfly robots.**

I. INTRODUCTION

The problem of trajectory tracking for underactuated robots has been addressed in a series of publications [1]–[6]. Most of these works focus on orbital stabilization, where the system state converges to a reference periodic trajectory up to a phase shift. This formulation has enabled the development of control algorithms that demonstrated effectiveness in real-world applications [7]–[10]. However, in some practical scenarios orbital asymptotic stability may be insufficient. For example, in cooperative or synchronized tasks involving multiple underactuated robots, asymptotic stability of the full state may be required, particularly when the robots share a common clock.

A straightforward approach to trajectory tracking is based on linearizing the tracking error dynamics and designing an LQR for the resulting linear time-varying (LTV) system. This method, described in Chapter 12 of [11], achieves asymptotic stability for small tracking errors and has been validated experimentally on a triple pendulum on a cart [12]. Compared to orbital stabilization methods, however, it is sensitive to initial time shifts and may lose stability if the robot becomes desynchronized.

Alternative approaches address synchronization of closed orbits by modifying orbital tracking algorithms to ensure coordination within a group of underactuated robots [2], [13]–[15]. For instance, [2] employs transverse linearization for a group of three robots to design a centralized controller that achieves synchronization. In [14], an ad hoc modification of the transverse linearization approach is proposed and validated experimentally on two robots.

[1]The authors are with Department of Information Technologies and AI, Sirius University of Science and Technology, Sochi, Russia, surov.m.o@gmail.com, mygrigorov@ya.ru, gusev.sv@talantiuspeh.ru, sumenkov.oy@talantiuspeh.ru

This work was supported by the grant of the state program of the "Sirius" Federal Territory: Scientific and technological development of the "Sirius" Federal Territory (Agreement No. 18-03 date 10/09/2024).

Our method for orbital stabilization with simultaneous time synchronization is a modification of orbital stabilization feedback based on the transverse linearization framework [2], [16]. For a given periodic trajectory, we augment the transverse dynamics with a desynchronization variable defined as the difference between physical time and the reference time corresponding to the "closest" point on the trajectory. We show that linearization of the extended transverse dynamics yields an LTV system that can be stabilized using a combination of LQR and sliding-mode control, similarly to [6], [17]. The resulting feedback law naturally decomposes into orbital stabilization and synchronization components. The synchronization term is bounded and includes the desynchronization variable through a signum function, preserving the advantages of orbital stabilization while ensuring bounded corrective actions even for large desynchronizations.

The remainder of the paper is organized as follows. Section II formulates the problem of periodic trajectory tracking for a class of nonlinear control systems. Section III reviews the orbital stabilization algorithm based on transverse linearization. The main results are presented in Section IV, where the transverse dynamics are extended with a desynchronization variable and two stabilization methods are proposed: an LQR design based on linearization of the extended dynamics and a sliding-mode control approach. Section V reports experimental results on a group of six Butterfly robots [18]. Concluding remarks are given in Section VI.

II. PROBLEM STATEMENT

We consider nonlinear control-affine systems of the form

$$\dot{x} = f(x) + g(x)\,u, \tag{1}$$

where $x \in \mathcal{X}$ is the state and $u \in \mathbb{R}^m$ the control input. The state space $\mathcal{X}$ is a smooth n-dimensional manifold; for Euler-Lagrange systems, it typically coincides with the tangent bundle $T\mathcal{Q}$ of a configuration manifold $\mathcal{Q}$. The functions f and g are continuously differentiable on $\mathcal{X}$.

System (1) is assumed to admit a smooth, nontrivial T-periodic solution

$$x_*(t) = x_*(t+T), \quad u_*(t) = u_*(t+T) \quad \forall t \in \mathbb{R}$$

satisfying $\frac{d}{dt}x_*(t) \equiv f(x_*(t)) + g(x_*(t))\,u_*(t)$. The trajectory $x_*(t)$ has no equilibria ($\dot{x}_*(t) \neq 0$ for all t) and no self-intersections. The associated orbit [11] is defined by

$$\gamma := \{x \in \mathcal{X} \mid \exists t : x = x_*(t)\}.$$

Under mild regularity conditions, γ is a smooth embedded submanifold of $\mathcal{X}$. For sufficiently small $\epsilon > 0$, we define the tubular neighborhood

$$U_\epsilon := \{x \in \mathcal{X} \mid \operatorname{dist}(x, \gamma) < \epsilon\},$$

where "dist" denotes the distance operator on $\mathcal{X}$.

In underactuated robots, the state typically consists of generalized coordinates and velocities, $x \equiv (q; \dot{q}) \in T\mathcal{Q}$, while the input u represents generalized forces, with $1 \leq \dim u < \dim q$. The periodic trajectory $x_*(t)$ therefore corresponds to a repetitive robot motion.

A fundamental problem in robotics [19] is to design a feedback law $u = u(t, x)$ such that $x(t)$ becomes a stable solution of the closed-loop system

$$\dot{x} = f(x) + g(x)u(t, x). \tag{2}$$

Depending on the application, different stability notions are relevant. For underactuated robots – such as bipedal walking mechanisms [3], [20] – local asymptotic orbital stability is most common, meaning that trajectories starting in U_ϵ converge to the orbit γ. Theoretically, a trajectory $x_1(t)$ then satisfies $x_1(t) - x_*(t - h) \to 0$ as $t \to \infty$ for some phase shift h. In practice, however, unmodeled dynamics and disturbances may cause $x_1(t)$ and $x_*(t)$ to drift apart even though $x_1(t)$ remains within U_ϵ.

Another class of control problems aims to design a feedback law ensuring asymptotic convergence of the tracking error $x - x_*(t) \to 0$ as $t \to \infty$. Although this formulation eliminates phase desynchronization, few ready-to-use algorithms are available [12], and existing asymptotic tracking methods are often less robust than those developed for orbital stabilization.

To overcome these limitations, we propose a control method that achieves asymptotic stability by modifying an orbital stabilization algorithm based on transverse linearization. For completeness, we briefly recall the main elements of this framework before introducing our modification.

III. TRANSVERSE LINEARIZATION APPROACH

A. Dynamics in Transverse Coordinates

A well-known approach to orbital stabilization is transverse linearization [1], [16], [21]. The key idea is to introduce local coordinates in a neighborhood of the reference orbit:

$$\theta = \pi(x) \in [0, T_\theta) \quad \text{and} \quad \xi = \alpha(x) \in \mathbb{R}^{n-1}, \tag{3}$$

where θ is the phase obtained by projecting x onto γ, and ξ collects the $n - 1$ transverse deviations. The transformation is assumed to be a diffeomorphism on U_ϵ, with inverse $x = \beta(\xi, \theta)$.

The projection π satisfies the monotonicity condition

$$\frac{d}{dt}\pi(x_*(t)) = \frac{\partial \pi(x_*(t))}{\partial x}\dot{x}_*(t) \geq \text{const} > 0 \ \forall t \in [0, T), \tag{4}$$

implying that $\theta_*(t) \equiv \pi(x_*(t))$ is strictly increasing and therefore can be extended continuously beyond one period as $\theta_*(t + kT) \equiv \theta_*(t) + kT_\theta$, $k \in \mathbb{Z}$. Hence the inverse $t = \theta_*^{-1}(\theta)$ exists, allowing the reparametrization

$$x_*(\theta) \equiv x_*\big(\theta_*^{-1}(\theta)\big), \quad u_*(\theta) \equiv u_*\big(\theta_*^{-1}(\theta)\big).$$

By a standard abuse of notation, x_* denotes both the original and reparametrized trajectories.

In coordinates ξ, θ, system (1) becomes

$$\dot{\xi} = f_\xi(\xi, \theta) + g_\xi(\xi, \theta)\, w \tag{5}$$

$$\dot{\theta} = f_\theta(\xi, \theta) + g_\theta(\xi, \theta)\, w \tag{6}$$

where the new control input w is defined by $w := u - u_*(\theta)$, and the functions $f_\xi(\cdot), f_\theta(\cdot), g_\xi(\cdot), g_\theta(\cdot)$ are given by

$$\begin{pmatrix} f_\xi(\xi, \theta) \\ f_\theta(\xi, \theta) \end{pmatrix} := J^{-1} f(\beta(\xi, \theta)) + J^{-1} g(\beta(\xi, \theta))\, u_*(\theta),$$

$$\begin{pmatrix} g_\xi(\xi, \theta) \\ g_\theta(\xi, \theta) \end{pmatrix} := J^{-1} g(\beta(\xi, \theta)). \tag{7}$$

The Jacobian $J := \frac{\partial \beta(\xi, \theta)}{\partial(\xi, \theta)}$ is invertible for sufficiently small ξ due to the local diffeomorphism between (ξ, θ) and x.

Dividing (5) by (6) yields the transverse dynamics in nonlinear form:

$$\frac{d\xi}{d\theta} = \frac{f_\xi(\xi, \theta) + g_\xi(\xi, \theta)\, w}{f_\theta(\xi, \theta) + g_\theta(\xi, \theta)\, w} =: \phi(\xi, \theta, w). \tag{8}$$

By the monotonicity condition (4), the denominator is strictly positive for sufficiently small ξ and w. Hence, within a sufficiently small tube U_ϵ, system (8) is well defined and locally equivalent to (1). The orbital stabilization problem therefore reduces to stabilizing the trivial solution $\xi(\theta) = 0$ of the transverse dynamics.

B. Orbital Stabilization Control Design

A common approach for stabilizing (8) is to linearize the right-hand side with respect to ξ and w (see [16], [21]):

$$\frac{d\xi}{d\theta} = A(\theta)\, \xi + B(\theta)\, w + o(\theta, \xi, w), \tag{9}$$

where the matrix functions $A(\theta) := \partial_\xi \phi(0, \theta, 0) \in \mathbb{R}^{(n-1)\times(n-1)}$ and $B(\theta) := \partial_w \phi(0, \theta, 0) \in \mathbb{R}^{(n-1)\times m}$ are T_θ-periodic, and $o(\xi, \theta, w)$ collects higher-order terms. If the linearized system (9) is controllable over one period [22], it can be stabilized with the feedback

$$w(\xi, \theta) = K(\theta)\, \xi. \tag{10}$$

using a T_θ-periodic gain matrix $K(\theta) \in \mathbb{R}^{m\times(n-1)}$. This defines a state feedback for the original system (1):

$$u(x) = u_*(\pi(x)) + K(\pi(x))\, \alpha(x). \tag{11}$$

Following [23], the control law (11) guarantees local asymptotic orbital stability of $x_*(t)$, but not asymptotic stability of the trajectory itself.

IV. TIME SYNCHRONIZATION ALGORITHM

A. Extended Transverse Dynamics

Below, we consider an extension of the transverse dynamics (8) that incorporates the robot's time desynchronization, expressed in terms of ξ, θ and w.

Let $x \in U_\epsilon$ be the state of the system at time t. Using the projection operator $\pi(x)$ and the alternative parametrization $\theta_*(t)$, the *robot's self-time* is defined as

$$\tau := \theta_*^{-1}(\pi(x)) + \nu T, \tag{12}$$

where $\nu \in \mathbb{N}$ counts the total number of periods completed by the robot. The controller is assumed to maintain an

internal state that tracks and updates ν. The robot *lateness* is then defined as

$$h := t - \tau. \tag{13}$$

While t normally represents physical time, rewriting the dynamics in terms of θ makes t a dynamic variable. Its evolution along a solution $\xi(\theta)$, $w(\theta)$ of (8) is given by (6) as

$$t = t_0 + \int_{\theta_0}^{\theta} \frac{1}{f_\theta\left(\xi\left(\varepsilon\right),\varepsilon\right) + g_\theta\left(\xi\left(\varepsilon\right),\varepsilon\right) w\left(\varepsilon\right)} d\varepsilon, \tag{14}$$

so that the dynamics of t now depend explicitly on ξ, θ and w.

Using the expressions in (6,8,12,13), the extended transverse dynamics can be written explicitly in terms of the variables ξ, θ and w as

$$\begin{aligned} \frac{d\xi}{d\theta} &= \frac{f_\xi\left(\xi,\theta\right) + g_\xi\left(\xi,\theta\right) w}{f_\theta\left(\xi,\theta\right) + g_\theta\left(\xi,\theta\right) w} \\ \frac{dh}{d\theta} &= \frac{1}{f_\theta\left(\xi,\theta\right) + g_\theta\left(\xi,\theta\right) w} - \frac{1}{\theta_*'\left(\theta_*^{-1}(\theta)\right)}, \end{aligned} \tag{15}$$

where the notation $\theta_*'(\tau) := \frac{d\theta_*(\tau)}{d\tau}$ used. It is straightforward to verify that (15) admits the trivial solution $\xi = 0$, $h = 0$, $w = 0$, corresponding to the reference trajectory $x_*(t)$, $u_*(t)$ of (1). The control objective is then to design a feedback law $w(\xi, h, \theta)$ that asymptotically stabilizes this trivial solution.

B. LQR Approach for Controller Design

As seen, system (15) represents a general nonlinear time-varying system. Its linear approximation is the LTV system

$$\frac{d\xi}{d\theta} = A_\xi\left(\theta\right)\xi + B_\xi\left(\theta\right) w, \;\; \frac{dh}{d\theta} = A_h\left(\theta\right)\xi + B_h\left(\theta\right) w \tag{16}$$

with T_θ-periodic matrices $A_\xi\left(\theta\right), A_h\left(\theta\right), B_\xi\left(\theta\right), B_h\left(\theta\right)$. If the system is controllable over one period [22], there exists an exponentially stabilizing feedback $w\left(\theta,\xi,h\right) = K_\xi\left(\theta\right)\xi + K_h\left(\theta\right)h$ with T_θ-periodic gains $K_\xi(\theta)$ and $K_h(\theta)$, computable via standard numerical methods [26]. This feedback yields a control law for the original nonlinear system (1):

$$u\left(t,x\right) = u_*(\theta) + K_\xi\left(\theta\right)\alpha\left(x\right) + K_h\left(\theta\right)\left(t-\tau\right). \tag{17}$$

A full proof of asymptotic stability of $x_*(t)$ in the closed-loop nonlinear system is beyond the scope of this work; we refer instead to the standard arguments in Theorem 4.13 of [11].

It is important to note, that the control law (17) guarantees local asymptotic stability only, i.e., for an initial state x_0 within a small neighborhood U_ϵ and small initial time deviation $\left|t_0 - \theta_*^{-1}(\pi\left(x_0\right))\right|$, the closed-loop solution converges to $x_*(t)$. Larger initial time deviations may compromise stability even if $x_0 \in \gamma$, so strict time synchronization can reduce the robustness benefits of orbital stabilization. One practical remedy is to saturate the lateness term:

$$u = u_*(\theta) + K_\xi(\theta)\,\xi + K_h(\theta)\,\mathrm{sat}\left(t-\tau, -h_{\max}, h_{\max}\right),$$

where $\mathrm{sat}(x, x_{\min}, x_{\max})$ limits x to $[x_{\min}, x_{\max}]$. While this modification may improve practical performance, it can potentially compromise stability from a theoretical standpoint. To address this issue, we propose an alternative sliding-mode control scheme in which the synchronization term remains bounded.

C. Sliding Mode Approach for Controller Design

The proposed synchronization method combines the LQR-based feedback w_{stab} for orbital stabilization (Section III-B) with a synchronization term w_{sync}, where the lateness variable h enters via a signum function. The total feedback for the extended dynamics (16) is

$$w := w_{\mathrm{stab}} + w_{\mathrm{sync}}, \quad \text{where} \quad w_{\mathrm{stab}} = K(\theta)\xi$$

ensures exponential stability of the ξ-subsystem, i.e., the trivial solution of

$$\frac{d\xi}{d\theta} = A_\xi\left(\theta\right)\xi + B_\xi\left(\theta\right)K\left(\theta\right)\xi =: A_1(\theta)\,\xi$$

is exponentially stable. Defining $A_2(\theta) := A_h(\theta) + B_h(\theta)K(\theta)$, the extended dynamics (16) become

$$\begin{aligned} \frac{d\xi}{d\theta} &= A_1(\theta)\xi + B_\xi(\theta)w_{\mathrm{sync}}, \\ \frac{dh}{d\theta} &= A_2(\theta)\xi + B_h(\theta)w_{\mathrm{sync}}. \end{aligned} \tag{18}$$

Consider a theorem, that provides a constructive method to stabilize system (18) for a single-input case $w_{\mathrm{sync}} \in \mathbb{R}$. The multi-input case can be formulated similarly, but its full statement and proof are omitted for brevity.

Theorem 1. *Consider the LTV system* (18) *with state* $\xi \in \mathbb{R}^{n-1}$, $h \in \mathbb{R}$, *and control input* $w_{\mathrm{sync}} \in \mathbb{R}$. *Assume:*

1) $A_1(\theta), A_2(\theta), B_\xi(\theta), B_h(\theta)$ *are continuous and* T_θ*-periodic,* $T_\theta > 0$.
2) *The uncontrolled subsystem* $\frac{d\xi}{d\theta} = A_1(\theta)\xi$ *is uniformly exponentially stable.*

Let $n(\theta) \in \mathbb{R}^{n-1}$ *be the unique* T_θ*-periodic solution of*

$$\frac{dn}{d\theta} = -A_1^\top\left(\theta\right)n - A_2^\top\left(\theta\right), \tag{19}$$

and define $b\left(\theta\right) := B_\xi^\top\left(\theta\right)n\left(\theta\right) + B_h\left(\theta\right)$, *such that* $|b\left(\theta\right)| \geq b_{\min} > 0\ \forall\theta$. *Then, for any* $k > 0$, *the feedback*

$$w_{\mathrm{sync}}\left(\theta,\xi,h\right) = -\frac{k}{b\left(\theta\right)}\mathrm{sign}\left(n^\top\left(\theta\right)\xi + h\right) \tag{20}$$

renders the equilibrium $\xi = 0$, $h = 0$ *of* (18) *globally asymptotically stable.*

The full proof of Theorem 1 is given in [27].

Remark 2. While the sliding variable $s := n^\top(\theta)\,\xi + h \neq 0$, the ξ-subsystem experiences the periodic disturbance $\pm\frac{kB_\xi(\theta)}{b(\theta)}$. Since the unforced system $\frac{d\xi}{d\theta} = A_1\left(\theta\right)\xi$ is exponentially stable, the forced system converges to a bounded steady state with amplitude $O(k)$. Consequently, for any sufficiently small $k > 0$ and prescribed $\epsilon > 0$, there exists $\delta > 0$ such that every trajectory of the original nonlinear closed-loop system starting within U_δ remains in U_ϵ for all $\theta \geq \theta_0$. This shows that the system stays close to the orbit γ while the synchronization term converges.

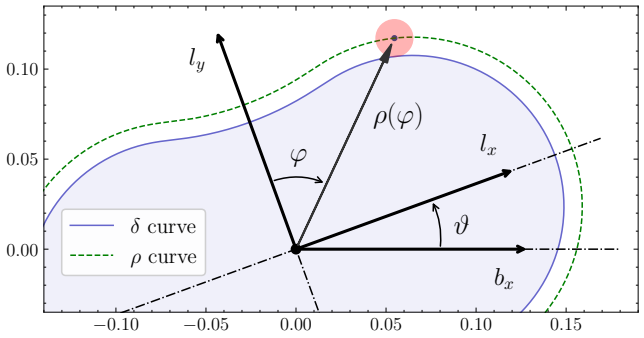

Fig. 1. Kinematics of the Butterfly robot. The angle ϑ defines the orientation of the link, while the angle φ specifies the position of the ball.

Using Theorem 1, the resulting control for system (1) is

$$u\left(t,x\right)=u_{*}(\theta)+K\left(\theta\right)\xi-\frac{k\cdot\operatorname{sign}\left(n^{\top}\left(\theta\right)\xi+h\right)}{n^{\top}\left(\theta\right)B_{\xi}\left(\theta\right)+B_{h}\left(\theta\right)}. \quad (21)$$

This feedback naturally decomposes into three components: the feedforward term $u_{*}(\theta)$, the orbital stabilization term $K\left(\theta\right)\xi$, and the bounded synchronization term $-\frac{k\cdot\operatorname{sign}\left(n^{\top}\xi+h\right)}{n^{\top}B_{\xi}+B_{h}}$. The magnitude of the synchronization term is limited by $k\sup_{\theta}\left|n^{\top}\left(\theta\right)B_{\xi}\left(\theta\right)+B_{h}\left(\theta\right)\right|^{-1}$ and can be made arbitrarily small by choosing a sufficiently small $k>0$, providing a tunable trade-off between orbit-tracking performance and the rate of lateness correction.

V. EXPERIMENTAL RESULT

The experimental platform is the Butterfly robot [18], a planar mechanical system consisting of a figure-eight-shaped link mounted to a fixed base via a single revolute joint. The link rotates in the vertical plane, driven by a DC motor, while a small spherical ball rolls passively along its surface. The link's angular position is measured by an encoder, and a vision system provides real-time estimates of the ball's position. This setup is used to validate nonprehensile manipulation algorithms, including tasks such as transporting the ball between prescribed equilibrium points and maintaining stable periodic motions [24].

Assuming ideal rolling and perfect spherical symmetry of the ball, together with the mechanism's rotational symmetry, the configuration space is topologically a torus. It is parameterized by two angles: ϑ, the orientation of the link relative to the base, and φ, the ball's position in a polar frame attached to the link (Fig. 1). The DC motor generates the control torque u at the link's revolute joint axis.

The robot represents underactuated mechanical system with two degrees of freedom and one control input. Dynamics of the robot are described by the Euler-Lagrange equations [17], which can be represented in the control-affine form (1) with state $x\equiv(\vartheta,\varphi,\dot{\vartheta},\dot{\varphi})^{\top}$ and scalar control input u as

$$\dot{x}=f(x)+g(x)u,\quad g(x),f(x)\in\mathbb{R}^{4}. \quad (22)$$

Exact expressions for the functions f and g are given in [17].

As shown in [10], the robot can perform one-directional periodic motions, where the ball rolls continuously along the link and the system returns to its initial configuration due to the topology of the configuration space. After one period $T=4.77$ sec, both the link orientation and ball position advance by 2π. We use this trajectory (Fig. 2) to illustrate the algorithm proposed in Section IV-C.

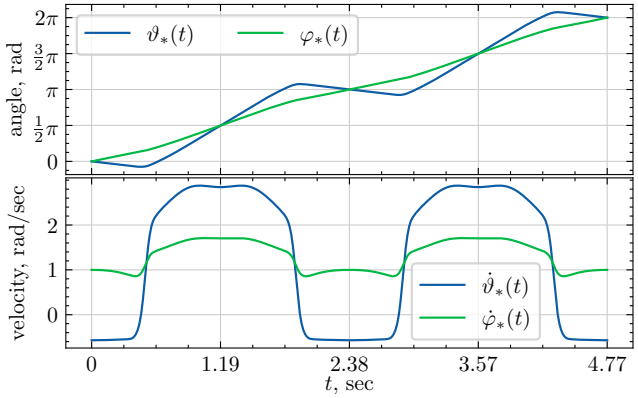

Fig. 2. Reference periodic trajectory of the Butterfly robot. The figure shows the generalized coordinates $\vartheta_{*}(t)\,,\varphi_{*}(t)$ and the corresponding generalized velocities $\dot{\vartheta}_{*}(t)\,,\dot{\varphi}_{*}(t)$.

A. Transverse Coordinates

As shown in Fig. 2, the coordinate $\varphi_{*}(t)$ is strictly increasing. This property motivates introducing the projection operator

$$\theta=\pi\left(x\right):=\varphi, \quad (23)$$

input transformation $w:=u-u_{*}\big(\varphi_{*}^{-1}(\varphi)\big)$ and the transverse coordinates $\xi=\alpha(x)\in\mathbb{R}^{3}$:

$$\begin{aligned}\xi_{1}&:=\vartheta-\vartheta_{*}\big(\varphi_{*}^{-1}(\varphi)\big)\,,\quad \xi_{2}:=\dot{\vartheta}-\dot{\vartheta}_{*}\big(\varphi_{*}^{-1}(\varphi)\big)\,,\\ \xi_{3}&:=\dot{\varphi}-\dot{\varphi}_{*}\big(\varphi_{*}^{-1}(\varphi)\big)\,.\end{aligned} \quad (24)$$

The linearization of the extended transverse dynamics (16) was carried out using formulas (7) and (15), together with the robot dynamics (22) and the transformations (23), (24). The resulting LTV system is T_{θ}-periodic with $T_{\theta}=2\pi$. Direct computation of the controllability Gramian over the interval $[0,2\pi]$ confirms that the linearized system is controllable over period. This fact allows the construction of an LQR for the subsystem $A_{\xi}(\theta)$, $B_{\xi}(\theta)$ with weighting matrices $Q=\operatorname{diag}\left(20,1,1\right)$ and $R=2\cdot10^{4}$. The stabilizing feedback gains $K(\theta)$ are found using the LMI approach [26].

The next step is to construct the synchronization term by computing the periodic solution $n\left(\theta\right)$ of (19). Reversing the argument, $\theta\mapsto-\theta$, renders this equation exponentially stable, so all solutions of the modified system converge to $n(-\theta)$. Thus, $n(-\theta)$ is computed numerically by integrating the modified equation from arbitrary initial conditions over several periods until the solution becomes effectively periodic. At this stage, all components required to implement the feedback law (21) are available.

B. Asymptotic Stabilization of the Robot Trajectory

The algorithm described above was tested on the physical robot. Fig. 3 shows the evolution of the lateness h, the transverse coordinates ξ and the rate of projection variable $\dot{\theta}$ as functions of physical time t.

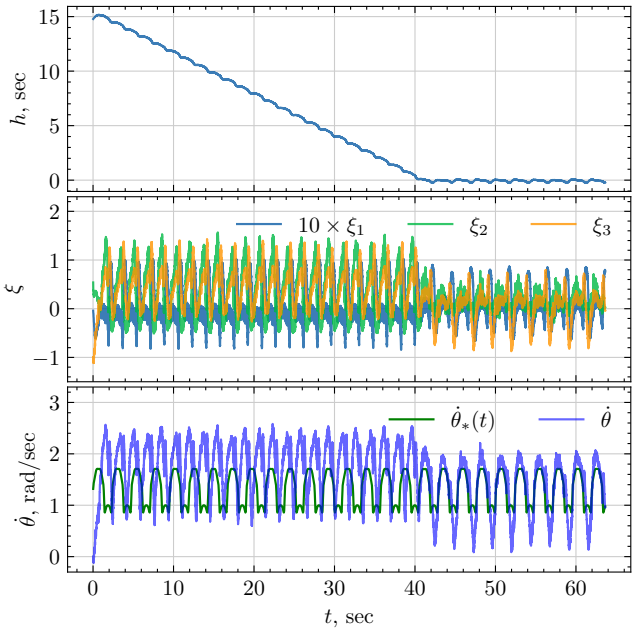

Fig. 3. Lateness of the robot h, transverse coordinates ξ and the rate of change of the projection variable $\dot{\theta}$.

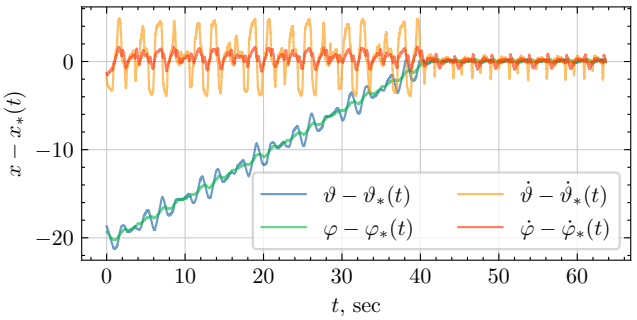

Fig. 4. Transient behavior of the tracking error $x - x_*(t)$.

The lateness h converges to zero at an approximately constant rate, despite an initial lateness of 15 sec, which is large relative to the trajectory period. The transverse coordinates ξ remain bounded but do not fully vanish due to unmodeled dissipation and variable delays of approximately 15 ms in the vision system. The projection parameter's rate $\dot{\theta}$ increases when lagging and decreases when catching up. Fig. 4 shows the deviation $x - x_*(t)$ approaching the origin and remaining within a small range, confirming practical asymptotic stability of the closed-loop system.

The control law (21) can also synchronize a group of robots sharing a common clock. Experimental results for the synchronization of two robots are shown in Fig. 5. Initially, the first robot lags behind the schedule while the second runs ahead. Both robots then converge to the reference trajectory $x_*(t)$. Once synchronization is achieved, the synchronization component of the control is manually disabled, while orbital stabilization remains active. The robots continue following their trajectories but gradually drift apart in time.

C. Decentralized Synchronization of Six Robots

We next evaluate decentralized synchronization using a heuristic modification of (21), replacing the reference physical time t with a reference time τ_* computed from other robots' self-times – either a neighbor or the average over all active robots. Although τ_* evolves differently from t and formal convergence is not guaranteed, the robustness of the sliding-mode feedback compensates for these differences, enabling network-level synchronization using only local time signals.

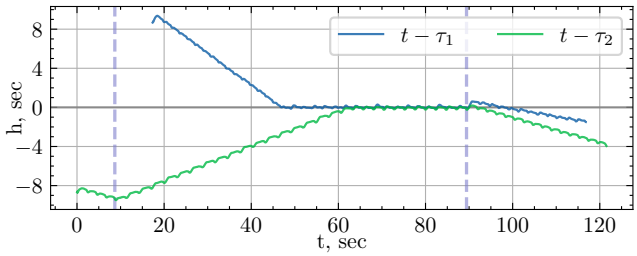

Fig. 5. Synchronization of two robots with respect to physical time. Dashed vertical lines indicate when synchronization is activated and deactivated.

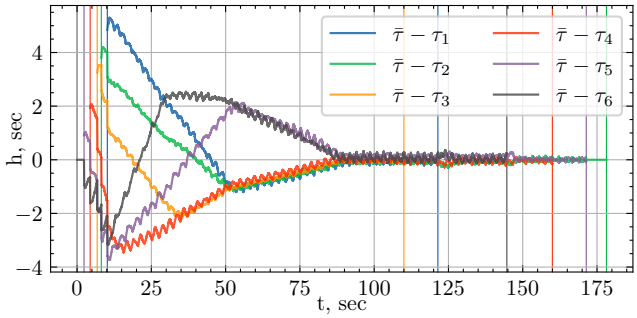

Fig. 6. Synchronization of six robots using neighbor-based references. The plot shows the lateness of each robot relative to the average self-time of all active robots, $\bar{\tau} := \frac{1}{N}\sum_i \tau_i$. Vertical lines indicate when robots were launched or stopped.

In the experiments, six robots are launched sequentially at varying intervals. Each robot publishes its self-time τ_i at 60 Hz and receives the self-times of all active robots. Based on the chosen scheme, each controller computes τ_* and the corresponding lateness $h_i = \tau_* - \tau_i$ for use in (21). Robots are manually switched off one by one, with the network automatically updating its active list. The remaining robots maintain synchronization, illustrating the decentralized operation of the scheme.

We tested several synchronization schemes inspired by coupled harmonic oscillators [25]. In the first scheme, each robot references only its immediate neighbor, so that the i-th robot's lateness is

$$h_i := \tau_{1+i \bmod N} - \tau_i, \quad i = 1..N,$$

forming a directed ring network. Fig. 6 shows the lateness of each robot relative to the average self-time of all active robots, with vertical lines marking robot activations and deactivations. Despite these sequential changes, the network achieves synchronization within finite time.

In the second scheme, the robots communicate over a complete directed graph, giving each controller access to the self-times of all active robots. The reference time is computed as the average self-time

$$\bar{\tau} := \frac{1}{N}\sum_i \tau_i, \quad h_i := \bar{\tau} - \tau_i, \quad i = 1..N.$$

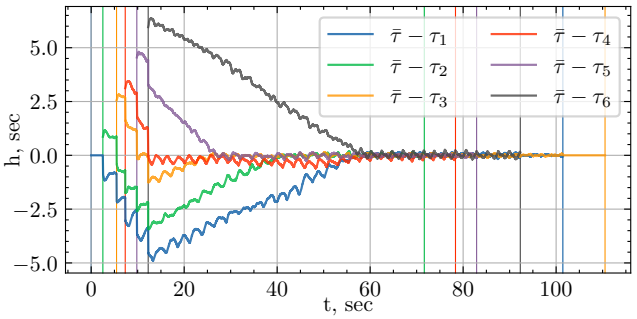

Fig. 7. Synchronization of six robots using average-based references. Each robot references the average of self-times of all active robots $\bar{\tau} := \frac{1}{N}\sum_i \tau_i$.

Experimental results are shown in Fig. 7, and a video is available at `https://youtu.be/WtvYQWtRSiw`.

VI. CONCLUDING REMARKS

We have presented a modification of the transverse-linearization approach that enables asymptotic stabilization of a reference periodic trajectory. The method combines the transverse framework with a sliding-mode technique, ensuring finite-time convergence of the time-desynchronization dynamics. The theoretical results have been validated experimentally, demonstrating the effectiveness of the proposed method not only for asymptotic stabilization of a single robot, but also for the design of decentralized control schemes for groups of robots.

Although the approach has been formulated for systems with an n-dimensional phase space and a single control input, it extends naturally to multi-input systems. A complete stability proof for the closed-loop nonlinear system under the proposed control law is beyond the scope of this conference paper and will be presented elsewhere. Likewise, a rigorous analysis of the proposed decentralized control schemes remains a subject of future work.

REFERENCES

[1] A. S. Shiriaev, J. W. Perram, and C. Canudas-de-Wit, "Constructive tool for orbital stabilization of underactuated nonlinear systems: Virtual constraints approach," IEEE Trans. Autom. Control, vol. 50, no. 8, pp. 1164–1176, Aug. 2005.

[2] A. S. Shiriaev, L. B. Freidovich, and S. V. Gusev, "Transverse linearization for controlled mechanical systems with several passive degrees of freedom," IEEE Trans. Autom. Control, vol. 55, no. 4, pp. 893–906, Apr. 2010.

[3] C. Canudas-de-Wit, B. Espiau, and C. Urrea, "Orbital stabilization of underactuated mechanical systems," in Proc. 15th IFAC World Congress, Barcelona, Spain, 2002, pp. 527–532.

[4] I. R. Manchester and J.-J. E. Slotine, "Transverse contraction criteria for existence, stability, and robustness of a limit cycle," Systems & Control Letters, vol. 63, no. 1, pp. 32–38, Jan. 2014.

[5] J. G. Romero, I. Gandarilla, V. Santibáñez, and B. Yi, "A constructive procedure for orbital stabilization of a class of underactuated mechanical systems," IEEE Trans. Control Syst. Technol., vol. 30, no. 6, pp. 2698–2706, Nov. 2022.

[6] C. F. Sætre, A. S. Shiriaev, L. B. Freidovich, S. V. Gusev, and L. M. Fridman, "Robust orbital stabilization: A Floquet theory–based approach," Int. J. Robust Nonlinear Control, vol. 31, no. 16, pp. 8075–8108, Nov. 2021

[7] B. G. Buss, K. A. Hamed, B. A. Griffin, and J. W. Grizzle, "Experimental results for 3D bipedal robot walking based on systematic optimization of virtual constraints," in Proc. IEEE Int. Conf. Robotics and Automation (ICRA), 2015, pp. 1234–1240,

[8] L. B. Freidovich, A. S. Shiriaev, and I. R. Manchester, "Experimental implementation of stable oscillations of the Furuta pendulum around the upward equilibrium," in Proc. 20th IEEE/RSJ Int. Conf. Intelligent Robots and Systems (IROS), San Diego, CA, USA, 2007, pp. 171–176.

[9] L. Freidovich, A. Robertsson, A. Shiriaev, and R. Johansson, "Periodic motions of the Pendubot via virtual holonomic constraints: Theory and experiments," Automatica, vol. 44, no. 3, pp. 785–791, Mar. 2008.

[10] M. Surov, A. Shiriaev, L. Freidovich, S. Gusev, and L. Paramonov, "Case study in non-prehensile manipulation: planning and orbital stabilization of one-directional rollings for the 'Butterfly' robot," in 2015 IEEE International Conference on Robotics and Automation (ICRA), Seattle, WA, USA, 2015, pp. 1484-1489,

[11] H. K. Khalil, Nonlinear Systems, 3rd ed. Upper Saddle River, NJ, USA: Prentice Hall, 2002. ISBN 978-0-13-067389-3.

[12] T. Glück, A. Eder, and A. Kugi, "Swing-up control of a triple pendulum on a cart with experimental validation," Automatica, vol. 49, no. 3, pp. 801–808, Mar. 2013.

[13] Y.-Y. Chen and Y.-P. Tian, "Formation tracking and attitude synchronization control of underactuated ships along closed orbits," Int. J. Robust Nonlinear Control, vol. 25, no. 16, pp. 3195–3200, Oct. 2015

[14] M. Surov, S. Pchelkin, A. S. Shiriaev, S. V. Gusev, and L. B. Freidovich, "On performing non-prehensile rolling manipulations: Stabilizing synchronous motions of Butterfly robots," in Proc. IEEE/RSJ Int. Conf. Intelligent Robots and Systems (IROS), Abu Dhabi, United Arab Emirates, 2024, pp. 12679–12685

[15] X. Xiang, C. Liu, L. Lapierre, and B. Jouvencel, "Synchronized path following control of multiple homogeneous underactuated AUVs," J. Syst. Sci. Complex., vol. 25, no. 1, pp. 71–89, Mar. 2012.

[16] S. Finet, L. Praly, Feedback Linearization of the Transverse Dynamics for a Class of One Degree Underactuated Systems, Proc. of the 54th IEEE Conference on Decision and Control, Osaka, Japan, 7802–7807, 2015.

[17] M. Surov, Sliding-Mode-Based Control Design for the Butterfly Robot, in IEEE Transactions on Control Systems Technology, doi: 10.1109/TCST.2026.3654633.

[18] K. M. Lynch, N. Shiroma, H. Arai, and K. Tanie, "The roles of shape and motion in dynamic manipulation: The butterfly example," in Proc. IEEE Int. Conf. Robotics and Automation (ICRA), Leuven, Belgium, 1998, vol. 3, pp. 1958–1963,

[19] B. Siciliano, L. Sciavicco, L. Villani, and G. Oriolo, Robotics: Modelling, Planning and Control, 3rd ed. London, U.K.: Springer-Verlag, 2009. ISBN 978-1-84628-641-4.

[20] E. R. Westervelt, J. W. Grizzle, C. Chevallereau, J. H. Choi, and B. Morris, Feedback Control of Dynamic Bipedal Robot Locomotion, 1st ed. Boca Raton, FL, USA: CRC Press, 2007.

[21] M. Surov, S. V. Gusev, and L. B. Freidovich, "Constructing transverse coordinates for orbital stabilization of periodic trajectories," in Proc. 2020 Amer. Control Conf. (ACC), Denver, CO, USA, 2020, pp. 836–841,

[22] V. A. Yakubovich, "A linear-quadratic optimization problem and the frequency theorem for periodic systems," Siberian Mathematical Journal, vol. 27, no. 4, pp. 181–200, 1986.

[23] G. A. Leonov, "Generalization of the Andronov–Vitt theorem," Regular and Chaotic Dynamics, vol. 11, no. 2, pp. 281–289, 2006.

[24] K. M. Lynch and M. T. Mason, "Dynamic nonprehensile manipulation: Controllability, planning, and experiments," International Journal of Robotics Research, vol. 18, no. 1, pp. 64–92, Jan. 1999.

[25] W. Ren, "Synchronization of coupled harmonic oscillators with local interaction," Automatica, vol. 44, no. 12, pp. 3195–3200, Dec. 2008.

[26] S. V. Gusev, S. Johansson, B. Kågström, A. S. Shiriaev, and A. Varga, "A numerical evaluation of solvers for the periodic Riccati differential equation," BIT Numerical Mathematics, vol. 50, no. 2, pp. 301–329, 2010.

[27] Surov Maksim, Orbital Stabilization and Time Synchronization of Unstable Periodic Motions in Underactuated Robots, 2025, doi:10.48550/arXiv.2509.20082